

<https://doi.org/10.1038/s42003-025-08109-5>

High efficiency rare earth element bioleaching with systems biology guided engineering of *Gluconobacter oxydans*



Alexa M. Schmitz^{1,4}, Brooke Pian¹, Sabrina Marecos¹, Mingming Wu¹, Megan Holycross², Esteban Gazel², Matthew C. Reid³ & Buz Barstow¹ ✉

Biological methods are a promising route for the environmentally-friendly production of rare earth elements (REE), which are essential for sustainable energy and defense technologies. In earlier work we identified the key genetic mechanisms contributing to the REE-bioleaching capability of *Gluconobacter oxydans* B58. Here we have targeted two of these mechanisms to generate a high-efficiency bioleaching strain of *G. oxydans*. Disruption of the phosphate-specific transport system through a clean deletion of *pstS* constitutively turns on the phosphate starvation response, yielding a much more acidic bioleachant, and increasing bioleaching by up to 30%. Coupling knockout of *pstS* with the over-expression of the *mgdh* membrane-bound glucose dehydrogenase gene using the P₁₁₂ promoter (strain *G. oxydans* Δ *pstS*, P₁₁₂:*mgdh*) reduces bioleachant pH by 0.39 units; increases REE-bioleaching by 53% at a pulp density of 10% and increases it by 73% at a pulp density of 1%.

Widespread implementation of sustainable energy technologies is essential for mitigating climate change¹. Rare earth elements (REE), including the lanthanides, yttrium, and scandium, are critical ingredients in many current sustainable energy technologies, such as wind turbine generators², solid-state lighting³, high-strength lightweight alloys^{4,5}, and battery anodes⁶; and future ones like high-temperature superconductors⁷.

However, the extraction of REE from ore has enormous environmental impacts^{8,9}. The first step in REE refining involves mining and comminution of ore, followed by gravity and/or magnetic separation to concentrate the REE-bearing solids. The REE-concentrate is then subjected to a strong leaching chemical, typically caustic soda or sulfuric acid (preferred for cost reasons), and then subjected to very high temperature and sometimes pressure as well to facilitate dissolution of metal ions⁸. These extraction steps result in disproportionate amounts of hazardous waste gas, water, and often radioactive waste (such as thorium from monazite ore)¹⁰.

A promising solution to the environmental impact of REE extraction is bioleaching^{11,12}. Bioleaching is already used commercially for the production of about 15% of the world's copper supply, 5% of gold, and small amounts of other metals¹³. Most of these processes depend on autotrophic (chemolithotrophic) microorganisms that oxidize ferrous iron or sulfur for energy, which in turn solubilizes the targeted metal ions¹⁴. REE-bioleaching typically uses heterotrophic microbes that convert sugars (glucose and/or agricultural

waste) into a bioleachant, a cocktail of solid matrix-dissolving compounds primarily composed of organic acids (at the time of writing the best characterized constituents are gluconic acid and 2–5-diketogluconic acid¹⁵, although in a companion article we identify genes that modulate the effectiveness of the bioleachant but do not meaningfully change the pH of the bioleachant¹⁶). Bioleaching of REE has been demonstrated at laboratory scale from a variety of solid sources, including concentrated virgin ore¹⁷, coal fly ash¹⁸, and recycled and end-of-life materials¹⁹.

Gluconobacter oxydans B58 is one of the most promising microorganisms for bioleaching REE^{19,20}. Reed et al.¹⁹ found that bioleachant made by *G. oxydans* was far more effective at bioleaching REE from spent fluid cracking catalyst (FCC) than gluconic acid alone. Techno-economic analysis of REE-bioleaching of spent FCC with *G. oxydans* demonstrated a small margin of profit, which is highly influenced by the cost of glucose and the efficiency of extraction²¹. Bioleaching efficiency can be improved by process factors including the pulp density of the REE source (the ratio of the REE-bearing solids mass to bioleachant volume); continuous vs. batch processing; and glucose concentration²¹. However, all of these factors also influence the process economics²².

Genetic engineering offers a promising approach to improving the efficiency of bioleaching processes without greatly affecting the process economics²³. Previously, we identified a comprehensive set of genes underlying organic acid production and REE-bioleaching efficiency by

¹Department of Biological and Environmental Engineering, Cornell University, Ithaca, NY, USA. ²Department of Earth and Atmospheric Sciences, Cornell University, Ithaca, NY, USA. ³School of Civil and Environmental Engineering, Cornell University, Ithaca, NY, USA. ⁴Present address: REEgen Inc., Ithaca, NY, USA.

✉ e-mail: bmb35@cornell.edu

generation and screening of a *G. oxydans* B58 whole genome knockout collection²⁴.

Our earlier work identified two important systems of genes that control REE-bioleaching efficiency. First, disruptions in single genes of the phosphate signaling and transport operon, including *pstS*, which encodes a phosphate signaling protein; and *pstC*, *pstA*, and *pstB*, which encode an ABC-type phosphate transporter, all produced large improvements in bioleaching efficiency²⁴.

Second, disruptions to genes involved in glucose oxidation to gluconic acid resulted in severe attenuation of bioleaching capabilities²⁴. Disruption of the *mgdh* gene that codes for the membrane-bound glucose dehydrogenase (mGDH) produced a 99% reduction in REE-bioleaching²⁴. Furthermore, disruption of *mgdh* results in a redirection of glucose into cellular metabolism and growth²⁰. Likewise, disruption of genes required for synthesis of the mGDH co-factor PQQ²⁵, including the *pqqABCDE* operon and *tldD* and *tldE* genes, also produces large reductions in REE-bioleaching in *G. oxydans*²⁴. Furthermore, previous work has demonstrated that over-expression of *mgdh* results in a several-fold increase in mGDH activity and production of organic acids²⁶.

Our objective was to improve bioleaching of REE by *G. oxydans* through genetic engineering. The results of the *G. oxydans* B58 whole genome knockout collection screen suggested a first roadmap for accomplishing this. We hypothesized that if we take the brakes off acid production by removing repression of phosphate-specific transport system signaling and increasing the incomplete oxidation of glucose into gluconic acid and other downstream acid products through the over-expression of *mgdh*²⁴, we could improve bioleaching. Here we present the results of targeted genome edits driving each modification, and the effect of their combination on the improvement of REE-bioleaching efficiency.

Results

Clean deletion of phosphate signaling and transport improves REE-bioleaching by up to 30.1%

The Pst phosphate-specific transport system is a transmembrane protein complex located in the bacterial inner membrane. The transmembrane subunits PstA and PstC bind to the periplasmic phosphate-binding protein, PstS, and to the cytoplasmic signaling protein, PstB²⁷. A screen of the *G. oxydans* B58 whole genome knockout collection for media-acidification through incomplete glucose oxidation found that transposon disruptions of

the *pstB*, *pstC*, and *pstS* genes increased acidification, and disruptions of *pstB* and *pstC* also increased REE-bioleaching²⁴.

As a transposon disruption does not always fully eliminate gene function, we first engineered clean deletion strains of *G. oxydans* B58 for *pstB*, *pstC*, and *pstS* ($\Delta pstB$, $\Delta pstC$, and $\Delta pstS$). These clean deletion strains were then grown to saturation, along with their corresponding transposon disruption strains from our *G. oxydans* knockout collection²⁴ ($\delta pstB$, $\delta pstC$, and $\delta pstS$), and wild-type *G. oxydans* B58 (wt), and mixed with glucose to produce an acidic biolixiviant. We refer to transposon disruption mutants with δ (lower case delta), and gene deletion mutants with Δ (upper case delta), as transposon insertions are likely to disrupt gene function, only a complete gene deletion guarantees loss of function. All six disruption and deletion strains had a longer lag period than wild-type when grown from a single colony. However, after back-dilution, this extended lag period disappeared for all three disruption strains, $\Delta pstB$ and $\Delta pstS$. All disruption and deletion strains generated significantly more acidic biolixiviants than wild-type *G. oxydans* (Fig. 1A). Biolixiviants produced by $\Delta pstB$ and $\Delta pstS$ were considerably lower in pH than those produced by the corresponding transposon disruption strains. We speculate that this is due to more complete disruption of the function of the phosphate-signaling and transport system, and greater deregulation of phosphate-solubilizing acid production. In contrast, biolixiviant produced by a clean deletion of *pstC* was slightly less acidic than that of the disruption strain. The growth rates of the wild-type *G. oxydans* and the $\Delta pstB$, $\Delta pstC$, and $\Delta pstS$ mutants are shown in Fig. S1. All of the *pst* deletion mutants show a long lag phase compared to wild-type, but achieve a slightly higher cell density. The $\Delta pstS$ mutant was chosen for further engineering as its cell density continues to increase beyond about 60 h, exceeding growth of $\Delta pstB$ and $\Delta pstC$, while the $\Delta pstB$ and $\Delta pstC$ mutants plateaued and start to decrease (Fig. S1).

Biolixiviant generated by each strain was then used for REE-bioleaching from a REE-concentrated allanite mineral ore. Biolixiviants produced by all three clean deletion strains were able to leach much more REE from the ore than wild-type (Fig. 1B). For the disruption strains, our results were similar to previous results²⁴, with the best performance coming from $\delta pstC$. As expected from the higher pH of its biolixiviant, $\Delta pstC$ did not produce additional bioleaching improvement. Biolixiviants produced by $\Delta pstB$ and $\Delta pstS$ both greatly outperformed those of their corresponding disruption strains at REE-bioleaching. $\Delta pstB$ raised bioleaching by 29.3% over wild-type, while $\Delta pstS$ raised bioleaching by 30.1%.

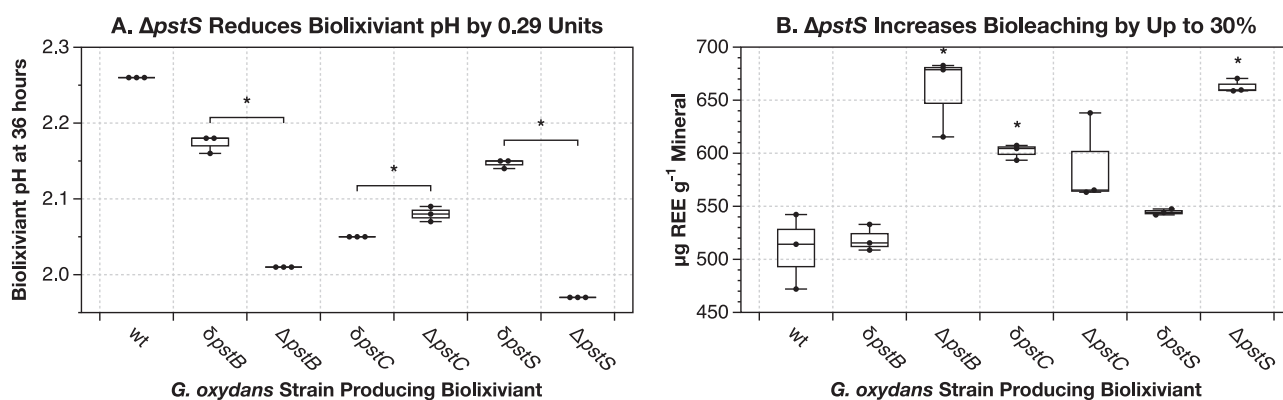


Fig. 1 | Deletion of the *pst* phosphate-specific transport genes drops biolixiviant pH by as much as 0.29 units, and improves bioleaching efficiency by up to 30.1% from allanite ore. A Effects of transposon disruption (δ) or deletion (Δ) of *pst* genes on the biolixiviant pH. Stars denote significant differences between disruption and deletion strains with a p -value < 0.01. The pH of the biolixiviants produced by all disruption and deletion strains was significantly different than wild type (wt) with p -values < 0.001. **B** Effects of disruption or deletion of *pst* genes on REE-bioleaching efficiency. Deletion of the ABC-type phosphate transporter ATP-binding protein

PstB increases bioleaching by 29.3% over wild-type. Meanwhile, deletion of the ABC-type phosphate transporter substrate-binding protein, PstS increases bioleaching by 30.1% over wild-type. Stars denote significant improvement in total REE-bioleaching as compared with wild-type *G. oxydans*, p < 0.05. For all experiments, strains were tested in triplicate, and results are demonstrative of multiple tests. Comparisons were made in Microsoft Excel with a two-tailed homoscedastic t -test. All data for this figure, including p -values, can be found in Supplementary Data S1⁴⁵.

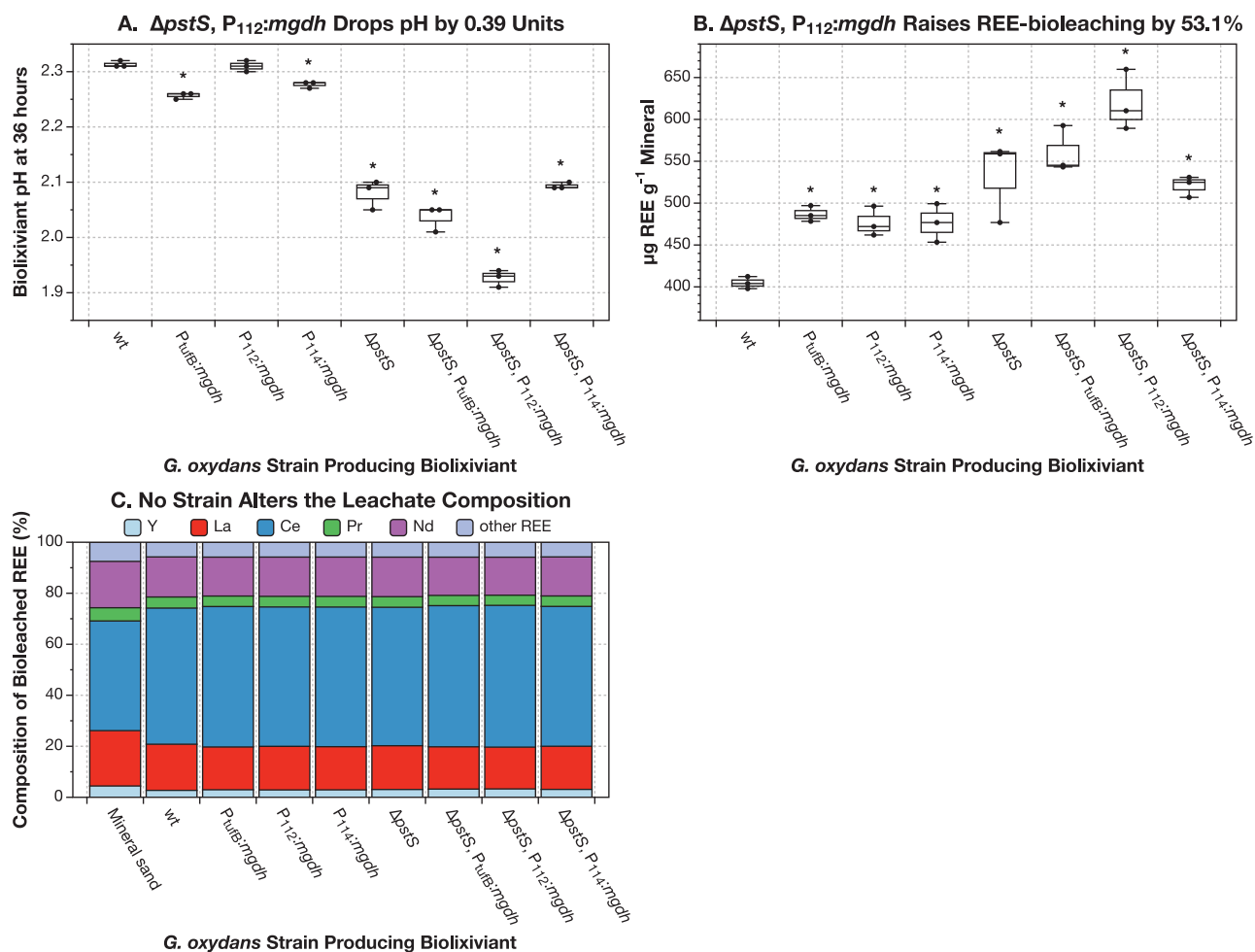


Fig. 2 | Over-expression of *mgdh* lowers biolixiviant pH by up to 0.39 units and increases REE-bioleaching from allanite ore by up to 53.1% at 10% pulp density. A Biolixiviant pH for all tested strains 36 h after glucose introduction. **B** Total REE extracted per gram of allanite sand for all strains. **C** Total contribution of the top five REE to the total REE extracted. A pulp density of 10% was used in all bioleaching

experiments (panels B and C; i.e., 10 g of allanite in 100 mL of biolixiviant). All tests were run in triplicate and are representative of multiple experiments. Stars denote significant difference compared with wild type (wt) *G. oxydans* by a two-tailed, homoscedastic *t*-test, $p < 0.05$. All data for this figure, including *p*-values, can be found in Supplementary Data S2⁴⁵.

Over-expression of membrane-bound glucose dehydrogenase in the $\Delta pstS$ background improves REE-bioleaching by up to 53.1%

We hypothesized that overexpression of *mgdh* would improve both media acidification and REE-bioleaching. To test this, we selected three promoter regions previously demonstrated to confer high expression on their downstream coding regions: the *tufB* promoter²⁸, and promoters P_{112} and P_{114} identified through an expression analysis of *G. oxydans* WSH-003^{29,30}. Each promoter was inserted upstream of the start codon for the *mgdh* coding region to create three *mgdh* over-expression strains: $P_{tufB}:mgdh$, $P_{112}:mgdh$, and $P_{114}:mgdh$. These insertions were also each combined with the *pstS* deletion, as it conferred the best combination of bioleaching and growth phenotypes of the three *pstS* deletion strains.

Clean deletion of *pstS* and over-expression of *mgdh* by the P_{112} promoter together had an additive effect on REE-bioleaching. In the wild-type *G. oxydans* background, over-expression of *mgdh* with the P_{tufB} and P_{114} high-activity promoters consistently produced a more acidic biolixiviant than wild-type, while over-expression of *mgdh* with P_{112} had no significant effect (Fig. 2A). But, in the $\Delta pstS$ background, $P_{112}:mgdh$ consistently yielded the most acidic biolixiviant of all three promoter insertion strains, lowering the pH by 0.39 units. Meanwhile, $P_{114}:mgdh$ yielded no improvement over $\Delta pstS$.

Biolixiviants produced by the $P_{tufB}:mgdh$, $P_{112}:mgdh$, $P_{114}:mgdh$ all produced higher REE-bioleaching than wild-type, but none were more

effective than $\Delta pstS$ (Fig. 2B). When combined with the $\Delta pstS$ background, $P_{tufB}:mgdh$ and $P_{114}:mgdh$ were no more effective than $\Delta pstS$ alone. But the combination of $\Delta pstS$ and $P_{112}:mgdh$ produced the most efficient REE-bioleaching strain tested (Fig. 2B). *G. oxydans* $\Delta pstS$, $P_{112}:mgdh$ produced REE-bioleaching that was 53.1% higher than wild-type. Taking a closer look at the leaching of each individual REE, we found that the overall composition of the leached metals did not vary between strains (Fig. 2C). This is reasonable as our mode of enhancing bioleaching primarily focuses on increased production organic acids that release most metals lodged in the mineral matrix rather than chelating REE selectively from the mineral. Even though the *G. oxydans* $\Delta pstS$, $P_{112}:mgdh$ mutant has a longer lag phase than the wild-type, it has improved growth kinetics compared with the other *pstS* deletion mutants (Fig. S1). Furthermore, the $\Delta pstS$, $P_{112}:mgdh$ mutant achieves even higher maximum cell density than the wild-type (Fig. S1).

Lowering the Pulp Density to 1% Raises REE-bioleaching by *G. oxydans* $\Delta pstS$, $P_{112}:mgdh$ to 73.1%

The overall efficiency of REE-bioleaching can be greatly influenced by a variety of process variables, most importantly the pulp density^{21,22}. To test how these variables affect the REE-bioleaching improvement conferred by genetic engineering, we compared the REE-bioleaching efficiency of *G. oxydans* $\Delta pstS$ and *G. oxydans* $\Delta pstS$, $P_{112}:mgdh$ at 1 and 10% pulp density of REE-containing mineral. Reducing the pulp density from 10 to 1% barely improved bioleaching by wild-type *G. oxydans*, if at all. However, the

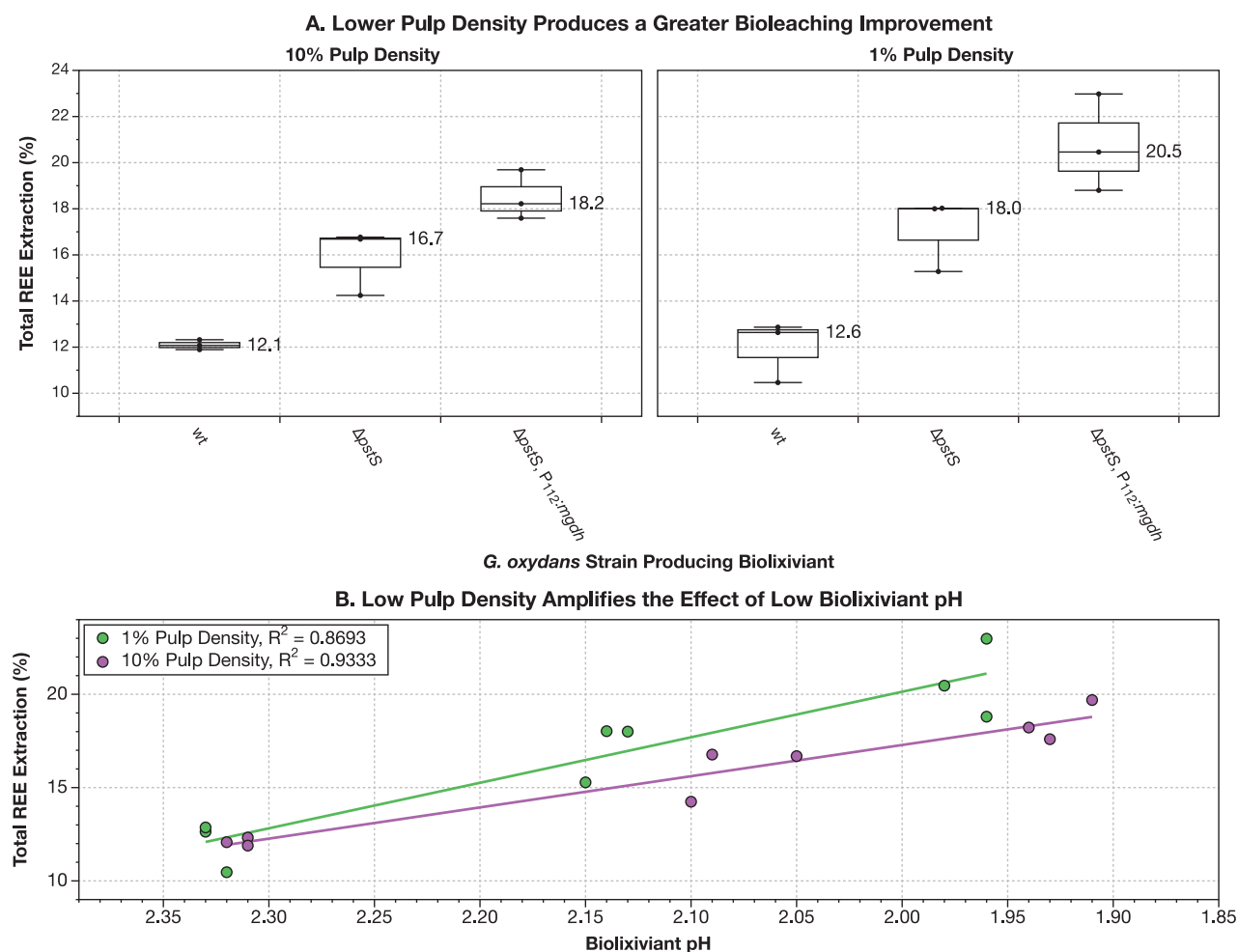


Fig. 3 | Up-regulating *mgdh* and knocking out *pstS* at the same time raises REE-extraction efficiency by up to 73.1% at low pulp density. A A comparison of percent total REE-extraction from allanite ore at 10% (left panel) vs. 1% (right panel) pulp density for wild-type *G. oxydans*, $\Delta pstS$, and $\Delta pstS, P_{112}:mgdh$. All strains were tested in triplicate. The median total REE extraction is reported next to each box and

whisker. **B** Correlation (green and purple lines) between biolixiviant pH and resulting percent total REE extracted at 1% (green dots) and 10% (purple dots) pulp density. All data for this figure, including *p*-values, mean, and median total REE extraction numbers, can be found in Supplementary Data S3⁴⁵.

bioleaching improvements of the engineered strains of *G. oxydans* were greater at the reduced pulp density. At 10% pulp density, *G. oxydans* $\Delta pstS, P_{112}:mgdh$ increased bioleaching over wild-type by 53% (Figs. 2B and 3A). But, at 1% pulp density *G. oxydans* $\Delta pstS, P_{112}:mgdh$ increased bioleaching over wild-type by 73.1% (Fig. 3B).

Previous work with *G. oxydans* bioleaching has indicated that biolixiviant pH is a good predictor of REE-bioleaching efficiency^{19,21,31}. A comparison of percent total REE extraction vs. biolixiviant pH demonstrates that the two are correlated, but the effect of lower pH is even stronger at the lower pulp density (Fig. 3B).

We compared the efficiency of bioleaching with the *G. oxydans* biolixiviant with neat nitric acid (Fig. S2). While the nitric acid extracts almost five times as much REE from allanite as the *G. oxydans* $\Delta pstS, P_{112}:mgdh$ biolixiviant (Fig. S2A), it extracts a slightly lower percentage of heavy REE than the biolixiviant (Fig. S2B), and is much more damaging to biological tissue (Figs. S3 and S4), and is not biodegradable.

Discussion

G. oxydans is an attractive candidate for the development of a high-efficiency rare earth bioleaching system. Through the incomplete oxidation of glucose, *G. oxydans* can rapidly produce a low pH biolixiviant that can be used for the solubilization of REE^{19,21,31}. Additionally, the recent development of several tools for genetic engineering in *G. oxydans* has greatly

increased the potential for improvement of commercially important applications^{29,30,32,33}. Here, we have taken advantage of this genetic versatility to greatly improve REE-bioleaching through genetic engineering in *G. oxydans* B58.

The greatest single impact on REE-bioleaching came from the disruption of the phosphate-specific transport system. Phosphate-solubilizing microbes (PSM) such as *G. oxydans* are able to unlock inorganic phosphate from minerals in the soil through the secretion of large amounts of organic acids³⁴. In *E. coli*, the deletion of *pst* genes removes repression of the *pho* regulon, resulting in a constitutive phosphate starvation response^{35,36}. One of the primary mechanisms of the phosphate starvation response is the up-regulation of enzymes involved in the release and scavenging of organic phosphates^{37,38}. Whether or not the *pho* regulon regulates genes in *G. oxydans* involved in the production of organic acids for mineral phosphate solubilization is still unknown, but it could explain the strong improvement of REE-bioleaching efficiency for *G. oxydans* *pst*-null strains.

Alternatively, a limiting factor for acid production in the wild-type bacteria may be intolerance of the increasingly acidic environment. Again in *E. coli*, the *pho* regulon has been shown to regulate genes underlying acid shock resistance, such as *asr*, which protects proteins in the periplasm from detrimental effects of low pH³⁹. If the low pH of the biolixiviant is limiting further acid production, an increase in acid shock resistance in the *pst* background would allow for greater production and a lower pH biolixiviant.

To directly target up-regulation of inorganic phosphate solubilization, and thus mineral bioleaching, we inserted high-expression promoter regions directly upstream of the *mgdh* gene, which is necessary for gluconic acid production from glucose²⁰. While the *tufB*, P_{112} , and P_{114} promoter regions have been reported to have high expression, this may not always hold true in the increasingly acidic environment that results from bioleaching production. We found that the three promoter regions did not perform similarly to each other, nor did they perform the same in the two different genetic backgrounds (wild-type vs. $\Delta pstS$) (Fig. 2A and B).

While all three *mgdh* promoter insertions improved REE-bioleaching in the wild-type background, only $P_{112}::mgdh$ had a significant effect when combined with the $\Delta pstS$ background. A possible explanation for this difference is a differential change in promoter activity between wild-type *G. oxydans* and $\Delta pstS$. Further work is needed to confirm if the increased acidification resulting from $P_{112}::mgdh$ in $\Delta pstS$ is a result of increased P_{112} promoter activity, which would indicate its regulation by *phoB*.

At the time of writing, we know that our genetic edits to *G. oxydans* affect the final pH of the bioleaching. However, we are not sure if this is because the edits simply change the concentration of the bioleaching (more of every component, while retaining their wild-type ratios) or change its composition. We intend to address this issue in an upcoming work.

Our genetic edits to *G. oxydans* allow us to maximize the effect of reducing mineral pulp density on bioleaching. By applying a design of experiment model, Deng et al.²² demonstrated that pulp density is the strongest contributor to the process economics of REE-bioleaching. Using available experimental results, Deng et al.²² predicted that the optimal pulp density for maximum yearly revenue would be 50%, despite this yielding the poorest percent REE extraction. This indicated that the higher REE-bioleaching efficiency at lower pulp densities does not outweigh the added cost of producing much greater volumes of bioleaching per unit of leached substrate.

By comparing percent REE bioleached to bioleaching pH (Fig. 3B), we were further able to demonstrate that driving the bioleaching pH down can have an even stronger effect with lower pulp density. Wild-type *G. oxydans* produces the same REE-bioleaching at 1 and 10% pulp density. At 10% pulp density, the $\Delta pstS$, $P_{112}::mgdh$ strain improved REE-bioleaching by 53% over wild-type. But, at 1% pulp density, the same strain improved bioleaching by 73%. As *G. oxydans* is an obligate aerobe⁴⁰, it requires oxygen for oxidation of glucose and production of bioleaching. We speculate that while bioleaching production by wild-type *G. oxydans* is not limited by oxygen availability, it is in the *G. oxydans* $\Delta pstS$, $P_{112}::mgdh$ strain. We further speculate that lowering the pulp density allows for better oxygen mass transfer, and hence better conversion of glucose to organic acids⁴¹.

Further modeling is needed to determine if such improvements would influence the ideal pulp density needed to maximize yearly revenue from REE-bioleaching.

Through genetic engineering of targeted mechanisms underlying acid production in *G. oxydans*, we have created a strain with greatly improved REE-bioleaching capability. Our highest performing strain, *G. oxydans* $\Delta pstS$, $P_{112}::mgdh$ performs up to 73% better at REE-bioleaching than wild-type. The global demand for rare earth elements is rising with the implementation of technological innovations, especially those related to renewable energy production, storage, and transmission⁶. With nearly all REE production taking place outside of the United States due to the cost of avoiding negative environmental impact⁹, the commercialization of a clean and sustainable, cost-competitive process for REE extraction is in high demand. REE-bioleaching with *G. oxydans* is done at room temperature and pressure and eliminates the need for massive amounts of harmful inorganic acids.

Although further improvements are still possible, such as up-regulation of genes contributing to PQQ synthesis, the $\Delta pstS$, $P_{112}::mgdh$ strain greatly improves on wild-type *G. oxydans* bioleaching capabilities, which are already expected to confer a margin of profit in commercial application^{21,42}. Furthermore, we have demonstrated how the modification of process parameters may further capitalize on the strain's bioleaching

improvements, thus more work is needed to understand the techno-economics. Ultimately, through the creation of a high-efficiency REE-bioleaching strain, we are a step closer to the development of a clean, sustainable REE production process capable of positively impacting the world REE market without the environmental expense. Furthermore, this development opens the prospect of developing environmentally-friendly leaching processes for other metals, including first row d-block metals (i.e., scandium to zinc), or precious metals (e.g., gold, silver, platinum, palladium, rhodium, ruthenium, iridium, and osmium).

Materials and methods

Genetic engineering of *G. oxydans*

In all experiments *G. oxydans* B58 (American Type Culture Collection, Manassas, VA) was cultured in yeast peptone mannitol (YPM; 5 g L⁻¹ yeast extract (C7341, Hardy Diagnostics, Santa Maria, CA), 3 g L⁻¹ peptone (211677, BD, Franklin Lakes, NJ), 25 g L⁻¹ mannitol (BDH9248, VWR Chemicals, Radnor, PA)) at 30 °C. All genetic modifications were made using the *codA*-based markerless gene deletion through homologous recombination and counter-selection with *codA* in the presence of *codB*⁴³.

For gene deletions, the 700 base pair genomic region directly upstream from the target gene's start codon and the 700 base pair genomic region directly downstream from the target gene's stop codon were cloned in tandem into the pKOS6b plasmid cut with XbaI using Gibson assembly⁴⁴ (E2611, New England Biolabs, Ipswich, MA). For insertion of promoter regions, 700 base pairs upstream and downstream from the target genes were cloned into pKOS6b, sandwiching the promoter region to be inserted. Primers used for all polymerase chain reactions to clone each plasmid are listed in Supplementary Data S4⁴⁵.

pKOS6b plasmids with homologous regions were transformed into *G. oxydans* following methods described in Mostafa et al.⁴⁶. Bacteria were grown from a single colony to an optical density between 0.8 and 0.9. Cells were harvested and washed three times with a half volume of HEPES, then resuspended in 250 μ L HEPES with 20% glycerol (Bluewater Chem Group, Fort Wayne, IN). Cells were flash frozen, then thawed on ice before transformation by electroporation with 2 kV on an Eppendorf Eporator. Transformed recombinant cells were recovered overnight in 1 mL EP medium (15 g L⁻¹ yeast extract, 80 g L⁻¹ mannitol, 2.5 g L⁻¹ MgSO₄·7H₂O (470301-684, Ward's Science, St. Catharines, ON, Canada), 0.5 g L⁻¹ glycerol, and 1.5 g L⁻¹ CaCl₂ (0556-500 G, VWR, Radnor, PA) then planted onto YPM agar supplemented with 100 μ g mL⁻¹ kanamycin (kan) (IB02120, VWR). Recombinants were selected and grown overnight in YPM supplemented with 100 μ g mL⁻¹ kan, then plated onto YPM supplemented with 60 μ g mL⁻¹ 5-fluorocytosine (5-FC) (TCF0321, VWR). Colonies that emerged were then transferred onto a new YPM 5-FC agar plate for clonal isolation. Colonies were isolated from several transfers and screened for recombinants with the desired mutation using colony PCR.

Bioleaching production and bioleaching

G. oxydans strains were grown by inoculating 2 mL YPM media with a single colony in a culture tube and grown for 48–72 h until the culture reached saturation. Bacterial culture was then back-diluted to an optical density of 0.05 in 10 mL YPM in a 250 mL Erlenmeyer flask, then grown for 24 h, shaking at 250 rpm. Culture was then divided into three 100 mL flasks by pipetting 3 mL into each, then 3 mL of 40% filter-sterilized glucose was added to each flask, resulting in a final glucose concentration of 20%. Culture and glucose were incubated for 24 h at 30 °C, shaking at 250 rpm to make the bioleaching. The bioleaching was then transferred to a 15 mL Falcon tube for pH measurement, after which 5 mL was transferred back into the same flask.

Unless otherwise specified, 500 mg REE-concentrated crushed allanite ore (Zappall from WRE) was added to each flask (10% pulp density, with the bioleaching described in the previous paragraph as the liquid phase), which was then vortexed on the highest setting until all solids were wet. Flasks were then incubated at room temperature and shaking at 200 rpm for 24 h to facilitate bioleaching. Solids were then briefly allowed to settle before 1 mL of

leachate was transferred to a 2 mL micro-centrifuge tube, which was then centrifuged for 1 min at top speed in a benchtop centrifuge to pellet any remaining solids. 500 mL of leachate was filtered through a 0.45 µm AcroPrep Advance 96-well filter plate (8029, Pall Corporation, Show Low, AZ, USA) by centrifugation at 1500×g for 5 min, then diluted 100-fold into 2% trace metal grade nitric acid (JT9368, J.T. Baker, Radnor, PA).

Samples were analyzed by an Agilent 7800 ICP-MS for all REE concentrations (*m/z*: Sc, 45; Y, 89; La, 139; Ce, 140; Pr, 141; Nd, 146; Sm, 147; Eu, 153; Gd, 157; Tb, 159; Dy, 163; Ho, 165; Er, 166; Tm, 169; Yb, 172; and Lu, 175) using a REE mix standard (67349, Sigma-Aldrich, St. Louis, MO) and a rhodium in-line internal standard (SKU04736, Sigma-Aldrich, St. Louis, MO, *m/z* = 103). Quality control was performed by periodic measurement of standards, blanks, and repeat samples. A pWT biolixiviant sample without bioleaching was spiked with 100 ppb REE standard and analyzed for all REE concentrations as a control. ICP-MS data were analyzed using the program MassHunter, version 4.5.

Measurement of growth curves for wild-type *G. oxydans* and engineered mutants

Growth curves for wild-type *G. oxydans* and engineered mutants (Fig. S1) were measured in 96-well polypropylene flat-bottom plates (Greiner Bio-One, 655261). The plates were sealed with optically clear Breathe-Easy seals (Diversified Biotech, BEM-1). Each well contained 150 µL of YPM medium. Optical density was recorded every 30 min using a BioTek Synergy 2 plate reader.

Statistics and reproducibility

Bench-scale bioleaching experiments with REE-concentrated crushed allanite ore were used to test each mutant strain's performance benchmarked against that of the wild-type. Biolixiviant pH was measured with an electrochemical pH meter, and rare earth element extraction levels in the bioleachate were measured by ICP-MS. To ensure quality control during ICP-MS analysis, periodic measurements of standards, blanks, and repeat samples were included. The data collected was analyzed using MassHunter, version 4.5. For all experiments, strains were tested in triplicate, and results are representative of multiple tests. Stars shown in Figs. 1–3 denote significant improvement in total REE-bioleaching as compared with wild-type *G. oxydans*, *p* < 0.05. Comparisons were made in Microsoft Excel with a two-tailed homoscedastic *t*-test. All *p*-values are exactly in Supplementary Data S1–S3 and S6.

Materials availability

Individual engineered strains of *G. oxydans* (up to ~10 at a time) are available at no charge for academic researchers. We are happy to supply a duplicate of the entire *G. oxydans* knockout collection to academic researchers, but we will require reimbursement for materials, supplies, and labor costs. Commercial researchers should contact Cornell Technology Licensing for licensing details. *E. coli* strains containing plasmids used for genetic modification of *G. oxydans* have been deposited at Addgene under accession codes 237501 (pKOS6b-pstB), 237502 (pKOS6b-pstC), 237503 (pKOS6b-pstS), 237504 (pKOS6b-URP112), 237505 (pKOS6b-URP114), and 237506 (pKOS6b-URtufB).

Reporting summary

Further information on research design is available in the Nature Portfolio Reporting Summary linked to this article.

Data availability

Source data underlying graphs generated and analyzed during the current study are included with this article and are available at <https://github.com/barstowlab/g.oxydans-double-mutant>. They are also archived on Zenodo⁴⁵.

Received: 29 June 2023; Accepted: 21 April 2025;

Published online: 27 May 2025

References

1. The Role of Critical Minerals in Clean Energy Transitions. (International Energy Agency, 2022).
2. Dent, P. C. Rare earth elements and permanent magnets. *J. Appl. Phys.* **111**, 07A721 (2012).
3. Nazarov, M. & Noh, D. *New Generation of Europium- and Terbium-Activated Phosphors*. (Pan Stanford Publishing, 2011).
4. Norman, A. F., Prangnell, P. B. & McEwen, R. S. The solidification behaviour of dilute aluminium–scandium alloys. *Acta Mater.* **46**, 5715–5732 (1998).
5. Adesina, O., Anzai, I. A., Avalos, J. L. & Barstow, B. Embracing biological solutions to the sustainable energy challenge. *Chemistry* **2**, 20–51 (2017).
6. Balam, V. Rare earth elements: A review of applications, occurrence, exploration, analysis, recycling, and environmental impact. *Geosci. Front.* **10**, 1285–1303 (2019).
7. Zurek, E. & Bi, T. High-temperature superconductivity in alkaline and rare earth polyhydrides at high pressure: A theoretical perspective. *J. Chem. Phys.* **150**, 050901 (2019).
8. Lucas, J., Lucas, P., Le Mercier, T., Rollat, A. & Davenport, W. *Rare Earths: Science, Technology, Production and Use*. (Elsevier Inc., 2014).
9. Eggert, R. et al. Rare Earths: market disruption, innovation, and global supply chains. *Annu. Rev. Environ. Resour.* **41**, 199–222 (2016).
10. Lucas, J., Lucas, P., Le Mercier, T., Rollat, A. & Davenport, W. in *Rare Earths* 47–67 (2015).
11. Mowafy, A. M. Biological leaching of rare earth elements. *World J. Microbiol. Biotechnol.* **36**, 61 (2020).
12. Rasoulina, P., Barthen, R. & Lakaniemi, A.-M. A critical review of bioleaching of rare earth elements: The mechanisms and effect of process parameters. *Crit. Rev. Env. Sci. Technol.* **51**, 378–427 (2020).
13. Johnson, D. B. Biomining—biotechnologies for extracting and recovering metals from ores and waste materials. *Curr. Opin. Biotechnol.* **30**, 24–31 (2014).
14. Barrie Johnson, D. & Hallberg, K. B. Carbon, iron and sulfur metabolism in acidophilic micro-organisms. *Adv. Microb. Physiol.* **54**, 201–255 (2009).
15. Dev, S. et al. Mechanisms of biological recovery of rare-earth elements from industrial and electronic wastes: a review. *Chem. Eng. J.* <https://doi.org/10.1016/j.cej.2020.124596> (2020).
16. Marecos, S. et al. Direct Genome-Scale Screening of *Gluconobacter oxydans* B58 for Rare Earth Element Bioleaching. *Commun. Biol.* **8**, 682 (2025).
17. Brisson, V. L., Zhuang, W.-Q. & Alvarez-Cohen, L. Bioleaching of rare earth elements from monazite sand. *Biotechnol. Bioeng.* **113**, 339–348 (2016).
18. Park, S. & Liang, Y. Bioleaching of trace elements and rare earth elements from coal fly ash. *Int. J. Coal Sci. Technol.* **6**, 74–83 (2019).
19. Reed, D. W., Fujita, Y., Daubaras, D. L., Jiao, Y. & Thompson, V. S. Bioleaching of rare earth elements from waste phosphors and cracking catalysts. *Hydrometallurgy* **166**, 34–40 (2016).
20. Krajewski, V. et al. Metabolic engineering of *Gluconobacter oxydans* for improved growth rate and growth yield on glucose by elimination of gluconate formation. *Appl. Environ. Microb.* **76**, 4369–4376 (2010).
21. Thompson, V. S. et al. Techno-economic and life cycle analysis for bioleaching rare-earth elements from waste materials. *ACS Sustain. Chem. Eng.* **6**, 1602–1609 (2018).
22. Deng, S. et al. Applying design of experiments to evaluate economic feasibility of rare-earth element recovery. *Proc. CIRP* **90**, 165–170 (2020).

23. Capeness, M. J. & Horsfall, L. E. Synthetic biology approaches towards the recycling of metals from the environment. *Biochem. Soc. Trans.* **48**, 1367–1378 (2020).
24. Schmitz, A. M. et al. Generation of a *Gluconobacter oxydans* knockout collection for improved extraction of rare earth elements. *Nat. Commun.* **12**, 6693 (2021).
25. Liu, D., Ke, X., Hu, Z.-C. & Zheng, Y.-G. Improvement of pyrroloquinoline quinone-dependent d-sorbitol dehydrogenase activity from *Gluconobacter oxydans* via expression of *Vitreoscilla* hemoglobin and regulation of dissolved oxygen tension for the biosynthesis of 6-(N-hydroxyethyl)-amino-6-deoxy- α -l-sorbofuranose. *J. Biosci. Bioeng.* **131**, 518–524 (2021).
26. Meyer, M., Schweiger, P. & Deppenmeier, U. Effects of membrane-bound glucose dehydrogenase overproduction on the respiratory chain of *Gluconobacter oxydans*. *Appl. Microbiol. Biotechnol.* **97**, 3457–3466 (2013).
27. Hsieh, Y.-J. & Wanner, B. L. Global regulation by the seven-component Pi signaling system. *Curr. Opin. Microbiol.* **13**, 198–203 (2010).
28. Saito, Y. et al. Cloning of genes coding for L-sorbose and L-sorbose dehydrogenases from *Gluconobacter oxydans* and microbial production of 2-keto-L-gulonate, a precursor of L-ascorbic acid, in a recombinant *G. oxydans* strain. *Appl. Environ. Microb.* **63**, 454–460 (1997).
29. Chen, Y. et al. Identification of gradient promoters of *Gluconobacter oxydans* and their applications in the biosynthesis of 2-keto-L-gulonate. *Front. Bioeng. Biotechnol.* **9**, 673844 (2021).
30. Qin, Z. et al. Repurposing the endogenous type I-E CRISPR/Cas system for gene repression in *Gluconobacter oxydans* WSH-003. *ACS Synth. Biol.* **10**, 84–93 (2021).
31. Antonick, P. J. et al. Bio- and mineral acid leaching of rare earth elements from synthetic phosphogypsum. *J. Chem. Thermodyn.* **132**, 491–496 (2019).
32. Fricke, P. M. et al. A tunable l-arabinose-inducible expression plasmid for the acetic acid bacterium *Gluconobacter oxydans*. *Appl. Microbiol. Biotechnol.* **104**, 9267–9282 (2020).
33. da Silva, G. A. R. et al. The industrial versatility of *Gluconobacter oxydans*: current applications and future perspectives. *World J. Microbiol. Biotechnol.* **38**, 134 (2022).
34. Rodríguez, H. & Fraga, R. Phosphate solubilizing bacteria and their role in plant growth promotion. *Biotechnol. Adv.* **17**, 319–339 (1999).
35. Wanner, B. L. & Chang, B. D. The *phoBR* operon in *Escherichia coli* K-12. *J. Bacteriol.* **169**, 5569–5574 (1987).
36. Vuppada, R. K., Hansen, C. R., Strickland, K. A. P., Kelly, K. M. & McCleary, W. R. Phosphate signaling through alternate conformations of the PstSCAB phosphate transporter. *BMC Microbiol.* **18**, 8 (2018).
37. Santos-Beneit, F. The *Pho* regulon: a huge regulatory network in bacteria. *Front. Microbiol.* **6**, 402 (2015).
38. Yuan, J., Wu, M., Lin, J. & Yang, L. Combinatorial metabolic engineering of industrial *Gluconobacter oxydans* DSM2343 for boosting 5-keto-D-gluconic acid accumulation. *BMC Biotechnol.* **16**, 42 (2016).
39. Sužiedėlienė, E., Sužiedėlis, K., Garbenčiūtė, V. & Normark, S. The Acid-Inducible *ars* Gene in *Escherichia coli*: transcriptional Control by the *phoBR* Operon. *J. Bacteriol.* **181**, 2084–2093 (1999).
40. Raspor, P. & Goranovic, D. Biotechnological applications of acetic acid bacteria. *Crit. Rev. Biotechnol.* **28**, 101–124 (2008).
41. Zhou, X., Zhou, X. & Xu, Y. Improvement of fermentation performance of *Gluconobacter oxydans* by combination of enhanced oxygen mass transfer in compressed-oxygen-supplied sealed system and cell-recycle technique. *Bioresour. Technol.* **244**, 1137–1141 (2017).
42. Jin, H. et al. Sustainable bioleaching of rare earth elements from industrial waste materials using agricultural wastes. *ACS Sustain. Chem. Eng.* **7**, 15311–15319 (2019).
43. Kostner, D., Peters, B., Mientus, M., Liebl, W. & Ehrenreich, A. Importance of *codB* for new *codA*-based markerless gene deletion in *Gluconobacter* strains. *Appl. Microbiol. Biotechnol.* **97**, 8341–8349 (2013).
44. Gibson, D. G. et al. Enzymatic assembly of DNA molecules up to several hundred kilobases. *Nat. Methods* **6**, 343–345 (2009).
45. Schmitz, A. M. Release of *G. oxydans* double mutant for submission. *Zenodo* <https://doi.org/10.5281/zenodo.8003432> (2023).
46. Mostafa, H. E., Heller, K. J. & Geis, A. Cloning of *Escherichia coli* *lacZ* and *lacY* genes and their expression in *Gluconobacter oxydans* and *Acetobacter liquefaciens*. *Appl. Environ. Microbiol.* **68**, 2619–2623 (2002).

Acknowledgements

We thank M. Weems at Western Rare Earths for advice and for the gift of allanite mineral sand. A.M.S. was supported by a Cornell Energy Systems Institute Postdoctoral Fellowship and a Small Grant from the Cornell Atkinson Center for Sustainability. This work was supported by Cornell University startup funds, an Academic Venture Fund award from the Atkinson Center for Sustainability at Cornell University, a Career Award at the Scientific Interface from the Burroughs Wellcome Fund to B.B., a gift from Mary Fernando-Conrad and Tony Conrad to B.B., an NSF-TIP award 2228821 to B.B. and A.M.S., and by ARPA-E award DE-AR0001341 to B.B., E.G., M.E.H., and M.W.

Author contributions

Conceptualization: A.M.S. and B.B.; Methodology: A.M.S. and B.B.; Investigation: A.M.S., B.P., S.M. and B.B.; Writing—Original Draft: A.M.S. and B.B.; Writing—Review & Editing: A.M.S., M.W., M.H., E.G., M.C.R., and B.B.; Funding acquisition: A.M.S., M.W., M.H., E.G., and B.B.; Resources: M.C.R., E.G., and B.B.; Supervision: M.W., M.H., E.G., M.C.R., and B.B.; Data Curation: A.M.S. and B.B.; Visualization: A.M.S. and B.B.; Formal Analysis: A.M.S.

Competing interests

A.M.S., B.P., and B.B. are pursuing patent protection for engineered organisms used for enhanced bioleaching (US provisional application 63/152,798). A.M.S. is CEO and co-founder of REEgen, Inc., which is commercializing REE biomining technology. The remaining authors declare no competing interests.

Additional information

Supplementary information The online version contains supplementary material available at <https://doi.org/10.1038/s42003-025-08109-5>.

Correspondence and requests for materials should be addressed to Buz Barstow.

Peer review information *Communications Biology* thanks Subhabrata Dev, Patrick Diep and the other, anonymous, reviewer(s) for their contribution to the peer review of this work. Primary Handling Editor: Ophelia Bu. A peer review file is available.

Reprints and permissions information is available at <http://www.nature.com/reprints>

Publisher's note Springer Nature remains neutral with regard to jurisdictional claims in published maps and institutional affiliations.

Open Access This article is licensed under a Creative Commons Attribution-NonCommercial-NoDerivatives 4.0 International License, which permits any non-commercial use, sharing, distribution and reproduction in any medium or format, as long as you give appropriate credit to the original author(s) and the source, provide a link to the Creative Commons licence, and indicate if you modified the licensed material. You do not have permission under this licence to share adapted material derived from this article or parts of it. The images or other third party material in this article are included in the article's Creative Commons licence, unless indicated otherwise in a credit line to the material. If material is not included in the article's Creative Commons licence and your intended use is not permitted by statutory regulation or exceeds the permitted use, you will need to obtain permission directly from the copyright holder. To view a copy of this licence, visit <http://creativecommons.org/licenses/by-nc-nd/4.0/>.

© The Author(s) 2025